Andrea Davila

Textural and Chemical Diversity of Plagioclase Phenocrysts

Honors Thesis

Thesis advisor: Dr. Adam Simon

28 April 2014

Abstract

This observational study compares the petrology of volcanic rocks from the Mutnovsky stratovolcano in southern Kamchatka to interpretations from the literature about volcanic rocks from similar tectonic settings. The analysis encompasses a range of rock types with bulk compositions ranging from basalt to rhyodacite. These rocks demonstrate textural and chemical diversity across the compositional range of samples as well as within individual samples. Quantitative data including point counts and microprobe traverses corroborate petrographic observations to reveal a potential scenario for Mutnovsky Volcano that can explain the observed textural and chemical diversity. Magma mixing and degassing induced-crystallization are two scenarios commonly invoked in the literature that may play a role at Mutnovsky Volcano. The samples from Mutnovsky Volcano exhibit characteristics that are consistent with both scenarios. For example, plagioclase grains in an andesite show swallowtail textures and large interior melt hollows that can be produced by diffusion-limited growth during large undercoolings when magmas degas. There are also coexisting euhedral and anhedral plagioclase grains within one sample, an observation that is interpreted to be consistent with the magma mixing hypothesis. Therefore, a comparison of the results from this study to those of various research groups investigating the evolution of arc volcanoes leads us to conclude that there is insufficient evidence to eliminate either of the two scenarios as a possible mechanism for producing rocks at Mutnovsky Volcano.

Introduction

Plagioclase is a ubiquitous mineral in the Earth's crust, existing in a variety of igneous rock types ranging from silica-poor basalts to silica-rich dacites and rhyolites. The prevalence of plagioclase in magmatic rocks, and its physical and chemical responses to changing pressure,

temperature and composition make it a particularly useful mineral for identifying sources of magmas and understanding magmatic evolution. Plagioclase often forms as euhedral phenocrysts and microphenocrysts; however, when plagioclase crystals develop as, for example, anhedral phenocrysts with disequilibrium textures, they capture important information about the processes they experienced prior to eruption. Plagioclase phenocrysts frequently capture melt inclusions, record growth zones, and develop a diverse set of textures and chemical compositions. Collectively, these features provide insight into subsurface processes.

Despite the usefulness of plagioclase in petrology, there is controversy within the scientific community about how to interpret the information provided by the mineral's textures and chemistry. Petrologists have not reached a consensus about what processes produce the zoning patterns, textures, and chemical diversity found in plagioclase phenocrysts. Therefore, the literature contains contradictory interpretations about the same observations of plagioclase, sometimes in the same rock sample. For example, Churikova et al. (2007) interpret the texture in figure 1 to indicate the resorption of plagioclase in a mixing zone due to a recharge of basaltic magma, whereas Johannes et al. (1994) presented a similar image (Figure 2), which Frey & Lange (2011) interpret to indicate the dissolution of a plagioclase xenocryst. In general, the current state of the literature for interpretations of plagioclase features can be more or less divided into two sets of opinions – one invoking magma mixing and another invoking degassing-induced crystallization.

Studies that support a magma mixing model often use geochemical data from plagioclase phenocrysts to support the hypothesis. For example, Churikova et al. (2007) studied major and trace element zoning patterns in plagioclase (Figure 3). They reported that the growth zones record changes in magma composition. Their interpretation is that the coexistence of chemically

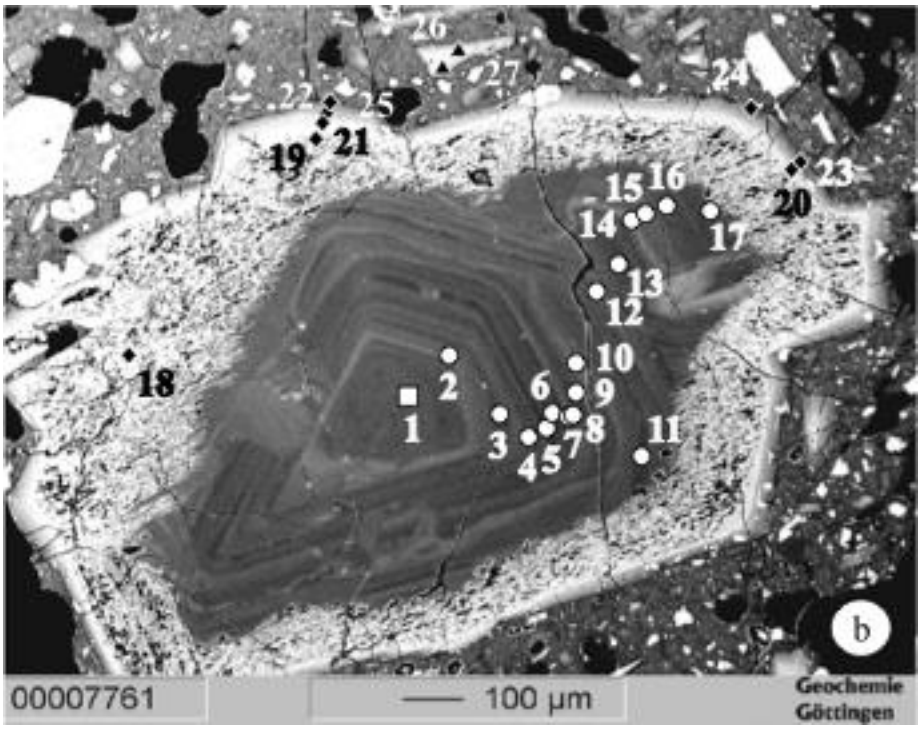

Figure 1: A photomicrograph of plagioclase texture observed by Churikova et al. (2007).

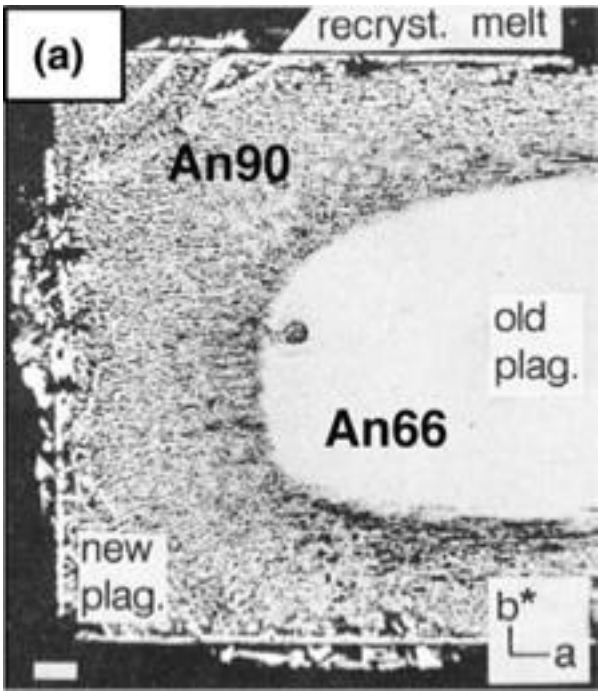

Figure 2: A photomicrograph of plagioclase texture observed in experiments by Johannes et al. (1994).

diverse plagioclase grains indicates that magma chamber evolution includes three processes: (1) crystal growth and fractionation; (2) mafic recharge and magma mixing, and (3) continued crystal growth in a freshly heated intermediate magma. One implication of this hypothesis is that mingling conceals the true chemical composition of the melt(s) from which volcanic rocks form (Reubi & Blundy, 2009). The origin of andesites has become a focal point for this controversy. Physical and chemical characteristics of plagioclase crystals, and the bimodal compositions of plagioclase-hosted melt, in andesites have been interpreted to record magma mixing (Reubi & Blundy, 2009).

In addition to plagioclase zoning patterns and melt inclusion compositions, crystal size distribution (CSD) plots and plagioclase textures are also interpreted to be evidence of magma mixing. For example, figure 5 from Innocenti et al. (2013), shows the population density of

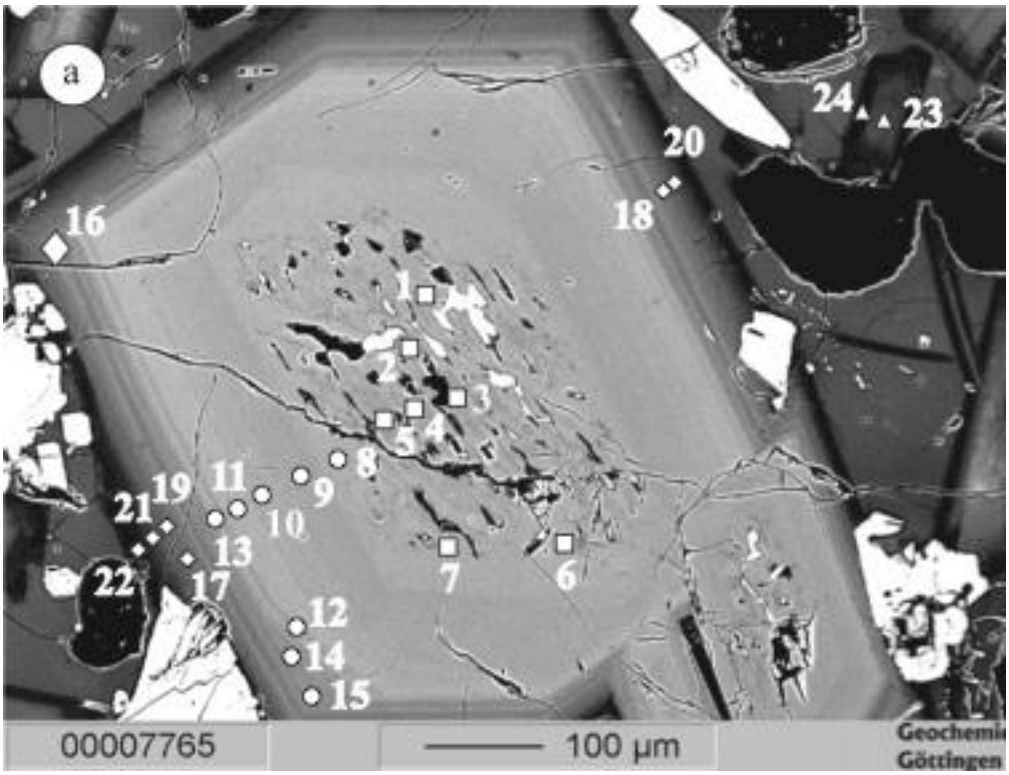

Figure 3: A photomicrograph of a sieved core and growth zones in a plagioclase phenocryst from Churikova et al. (2007).

plagioclase as a function of crystal size range. These authors highlight a kink in the slope of the line that describes their measured CSD. They interpret the kink to indicate two distinct populations of plagioclase, which the authors suggest represent resorption events. The resorption events, which may be a result of an injection of new magma, are manifested in disequilibrium textures, such as sieved cores (Figure 3), and reverse zoning observed in plagioclase grains.

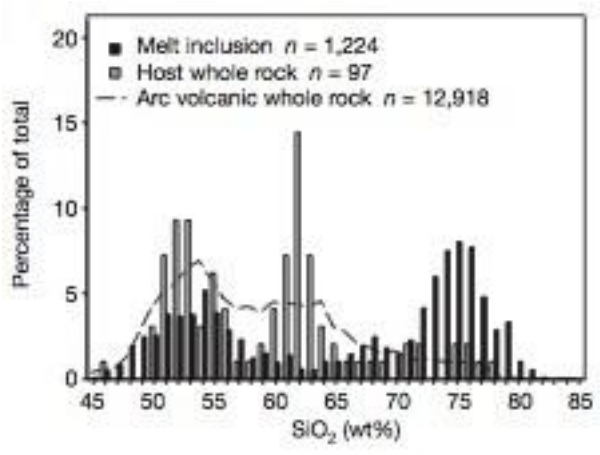

Figure 4: A graph showing the compositional distribution of melt inclusions from Reubi & Blundy (2009).

Magma mingling is commonly invoked as the cause for formation of intermediate composition magmas in arc environments; however, other plausible mechanisms that have been proposed to explain observations of plagioclase merit and warrant investigation. The broader scientific community agrees that large stratovolcanoes produce a wealth of texturally and compositionally diverse, phenocryst-rich rocks, and that magma mixing is an important process for producing the rocks in this tectonic setting. Nevertheless, some studies question the role that magma mixing plays at peripheral vents, arguing instead that diverse plagioclase compositions and textures may develop owing to changes in melt water concentration via degassing-induced crystallization (Crabtree & Lange, 2010). Consequently, scientists have proposed alternative processes to explain textural and chemical diversity plagioclase.

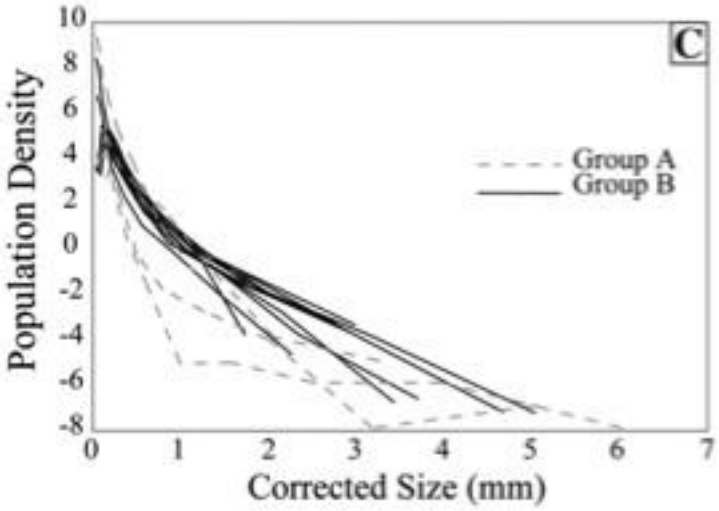

Figure 5: A CSD plot from Innocenti et al. (2013). Here they divide the plagioclase into two populations. Group A samples are from basalts and group B samples come from basaltic andesites.

Although zoning is prevalent in many plagioclase grains, experiments by Lofgren (1974), Hammer & Rutherford (2002) and Suzuki et al. (2007) demonstrate that the sodic component of the grain frequently crystallizes after the calcic component; i.e., normal zoning. One alternative process that explains the reverse zoning seen in plagioclase occurs when the rim of a plagioclase phenocryst crystallizes first, creating a hollow channel that later crystallizes inward. Furthermore, experimental simulations demonstrate that diverse plagioclase textures, including swallowtail and hopper textures, can occur via degassing-induced crystallization (Hammer & Rutherford, 2002; Couch et al., 2003; Martel & Schmidt, 2003; Szramek et al., 2006; Suzuki et al., 2007).

The purpose of this study is to investigate and understand the processes that produce the diverse set of plagioclase textures and compositions found in basalts, basaltic andesites, andesites, and dacites. To do so this study analyzes samples from a stratovolcano by using a variety of both qualitative and quantitative techniques, including petrographic observations, point

counting, Scanning Electron Microscopy (SEM), and electron probe microanalyses (EPMA). Finally, the observations and data are synthesized and compared and contrasted to the results of published studies with conflicting interpretations.

Geologic Setting

The samples used for this study were collected from Mutnovsky Volcano in Kamchatka. Mutnovsky is an active arc-front volcano located on the Kamchatka Peninsula in Eastern Russia (Figure 6: Moore et al.1992). The following geologic description for Mutnovsky is based on Selyangin (1993). Mutnovsky Volcano consists of four overlapping eruptive centers – stratocones known as Mutnovsky I, II, III, and IV (Robertson et al., 2013). A cross section of the volcano is provided in figure 7.

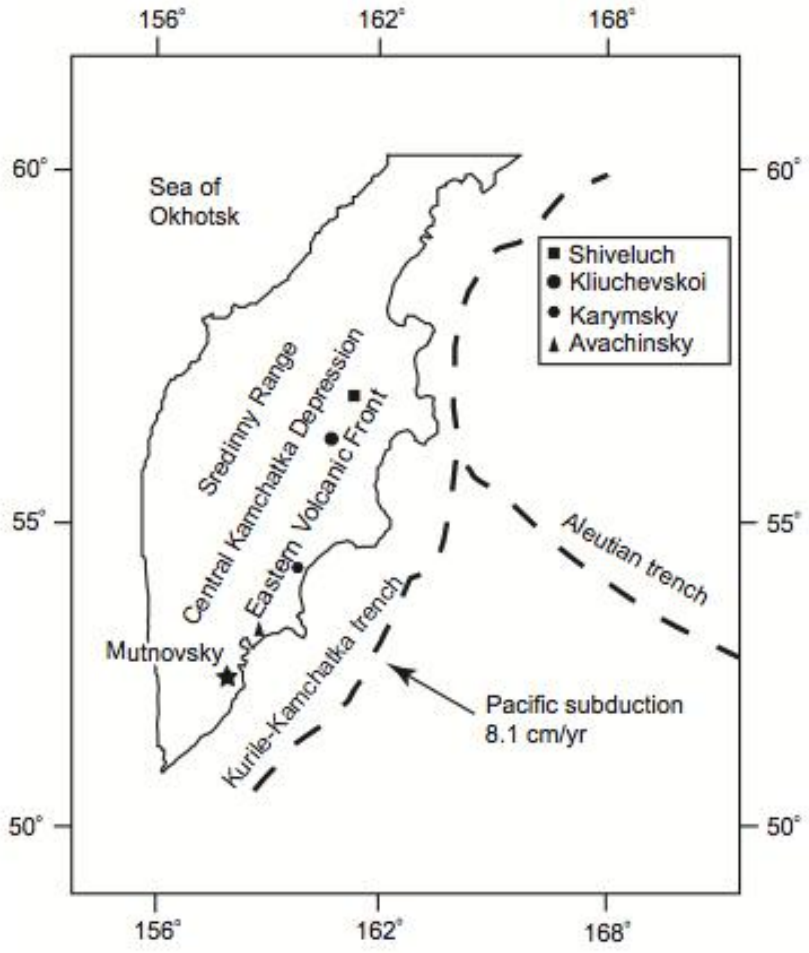

Figure 6: A regional map of Kamchatka showing the location of Mutnovsky Volcano; Moore et al. (1992) calculated the subduction rate.

The development of the stratocones is thought to proceed in cycles (Selyangin 1993). The cycle begins with the northwest subduction of the Pacific Plate and the growth of a new cone. Next, a large crater forms, and a cone grows within the caldera. Finally eruptive activity ceases, and the vent shifts, beginning a new cycle. Mutnovsky I is the oldest cone of the four.

Mutnovsky I, II and III erupted magmas ranging from basalt to rhyodacite; however, the majority of the volcanic rocks at these centers are basalts and basaltic andesites, while the more silica-rich lavas are relatively volumetrically sparse (Robertson, 2013). Mutnovsky IV, the youngest and lowest cone, has the least variable composition, producing purely basalts and basaltic andesites.. This study focused on samples from Mutnovsky I, II and III.

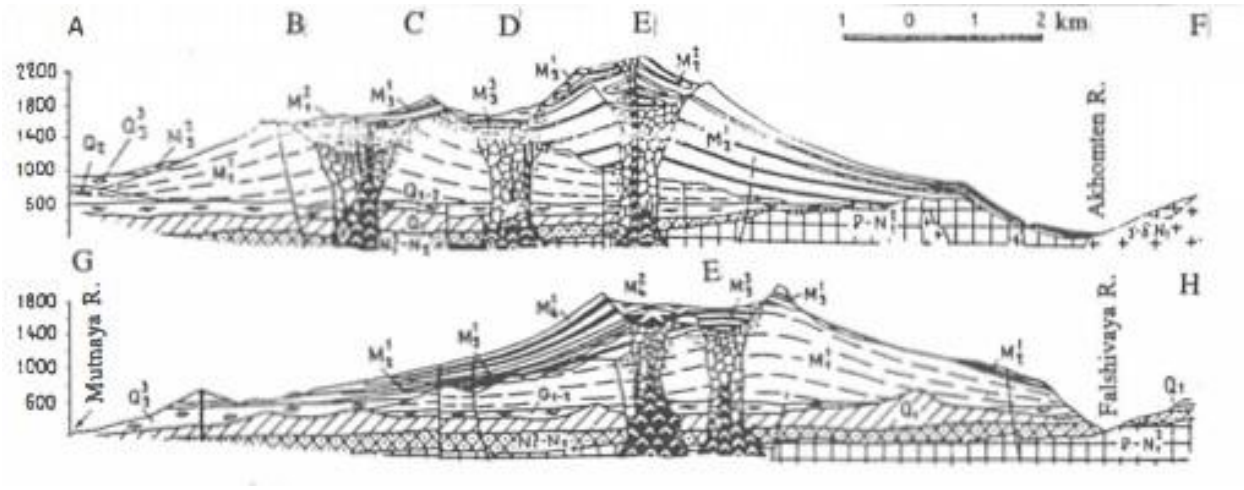

Figure 7: A cross-section of Mutnovsky volcano showing the relative positions of the four cones from O.B. Selyangin (1993).

Methods

Samples were collected from each of Mutnovsky's eruptive centers (MI, MII, MIII, and MIV) along with rock chemistry data and thin sections for each of the samples. Petrographic observations of various rock types with bulk compositions ranging from basalt to rhyodacite are presented. The observations focus on alterations on the faces and along fractures of plagioclase phenocrysts, melt inclusions, the fabric of the inclusions, plagioclase zoning, and crystal form. Chemical data obtained by using the SEM and EPMA, normative mineralogy calculations (CIPW), and point counting are used to expand on the petrographic observations.

Results

Table 1 includes whole rock chemistry, CIPW norms, and point counting results. Note that the rock chemistry and CIPW data are provided in weight percent. Point counting was performed by using a polarized light microscope to identify the mineral at the center of the optical cross hairs for 1000 points per thin section, and results are provided in terms of percent of the total number of counts. The boundary between phenocryst and microphenocryst size is 200 microns.

Mutnovsky I

Sample CM-33 comes from a hypocrystalline (a volcanic rock consisting of glass and crystals), medium to coarse-grained basalt with a crystalline groundmass (56.5%) containing glass, vesicles and phenocrysts. Phenocrysts include plagioclase (35.1%) and pyroxenes (1.3%). The sample contains both euhedral plagioclase as well as subhedral to anhedral plagioclase. The euhedral plagioclase are often large phenocrysts with optical zoning and inclusions (Figure 9). All of the plagioclase grains analyzed in this sample are normally-zoned; a representative EPMA chemical traverse is provided in figure 8. The anhedral plagioclase occur both as large

Cone #	3	1	1	1	2	1	2	3
Rock type	Basalt	Basalt	B. Andesite	Andesite	Andesite	Dacite	Rhyodacite	Dacite
Analysis	Whole rock							
Sample #	M3-08-08	CM-33	M1-06-08	CM-24	CM-147	CM-47	CM-113	CM-8a
SiO_2	48.85	51.56	53	59.36	59.88	64.68	67.53	69.4
Al_2O_3	22.65	22.55	17.26	17.87	16.33	16.04	14.63	14.61
FeO (T)	7.14	7.39	10.58	6.06	7.27	5.34	4.72	3.65
MnO	0.131	0.21	0.224	0.16	0.16	0.15	0.108	0.1
MgO	4.4	3.18	3.43	2.18	1.96	1.62	1.05	0.75
CaO	12.42	8.56	8.06	5.46	4.74	4.02	3.31	3.09
Na_2O	2.16	2.82	3.43	4.32	4.63	3.76	4.55	4.18
K_2O	0.28	0.59	0.44	1.02	1.51	1.98	2.1	3.18
TiO_2	0.59	1.04	1.31	1.01	1.26	0.91	0.47	0.63
P_2O_5	0.09	0.15	0.26	0.31	0.45	0.22	0.1	0.12
LOI	0.63	1.48	1.41	1.12	0.96	0.85	0.21	0.26
Total	100.1	100.35	100.6	99.55	99.96	100.16	99.33	100.33
Analysis	CIPW							
Sample #	M3-08-08	CM-33	M1-06-08	CM-24	CM-147	CM-47	CM-113	CM-8a
Quartz	0	5.13	5.66	12.19	10.82	21.25	21.8	23.69
Plagioclase	69.56	65.35	59.42	61.62	58.49	50.32	51.79	47.08
Orthoclase	1.65	3.49	2.6	6.03	8.92	11.7	12.41	18.79
Corundum	0	2.07	0	0.47	0	0.93	0	0
Diopside	8.08	0	0.32	0	1.07	0	2.12	2.43
Hypersthene	15.35	19.15	24.6	14.36	14.91	11.87	8.97	5.98
Olivine	2.2	0	0	0	0	0	0	0
Ilmenite	1.12	1.98	2.49	1.92	2.39	1.73	0.89	1.2
Magnetite	0.58	0.59	0.86	0.49	0.58	0.43	0.38	0.29
Apatite	0.21	0.35	3.27	0.72	1.04	0.51	0.23	0.28
Analysis	Point count							
Sample #	M3-08-08	CM-33	M1-06-08	CM-24	CM-147	CM-47	CM-113	CM-8a
Plag	30.8	35.1	17.8	24	12	11.4	13.7	11.7
Pyroxene	0	0	1	6.3	0.4	2.8	1.7	1.1
Olivine	3.4	1.3	0	0	0	0	0	0
Qtz	0	0	0	0	0	0.9	1.6	0.5
Amphibole	0	0	0	0	0	0	0	0
Oxides	0	0	0	2	0	0	0	0
Groundmass	65.4	56.5	80	63.1	87.2	82.3	80.7	85.4
Vesicle	0.1	7.1	1.1	0.1	0.4	2.2	2	1
Unknown	0.3	0	0.1	0	0	0.4	0.3	0.3

(i.e., > 1000 microns) and small phenocrysts (i.e., <500 microns), and they often have mottled inclusions or ratty boundaries (Figure 10).

When present, the melt inclusions in plagioclase associated with euhedral phenocrysts cluster in bands that reflect the shape of the growth zones, especially near the boundary of the crystal. These inclusions are small and spherical. Other inclusions are large with irregular shapes, sometimes forming networks with other inclusions on the crystal face. These inclusions are typically found in anhedral to subhedral phenocrysts in the sample.

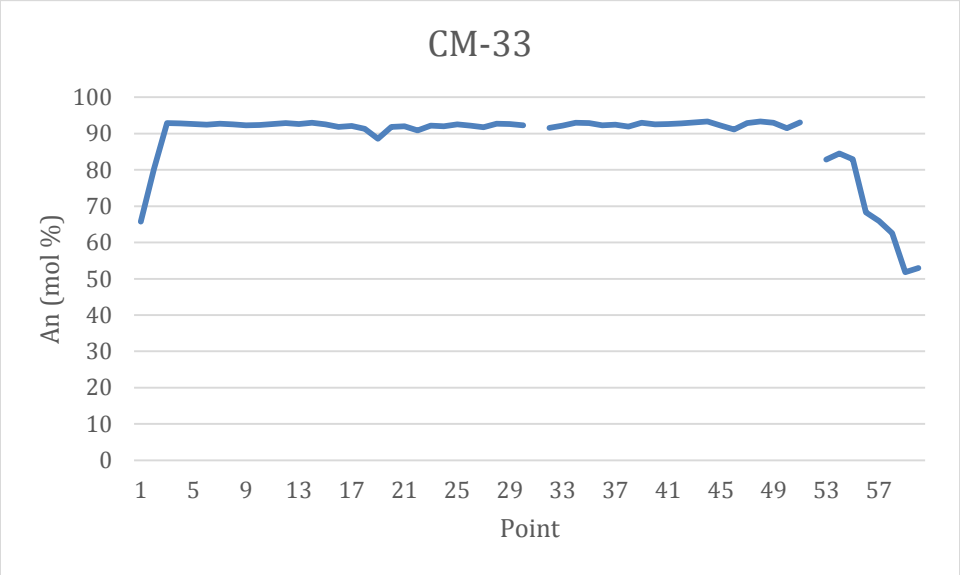

Figure 8: In CM-33, a plagioclase traverse reveals a calcic core and a relatively sodic rim i.e. a normally-zoned grain. Note this is not the same grain as in figure 6.

Sample CM-47 is a medium to coarse-grained dacite with porphyritic, hypocrystalline texture. This dacite consists of plagioclase (11.4%) and pyroxene (2.8%) phenocrysts and a crystalline and glassy groundmass (82.3%). There are also several glomerocrysts (aggregates of crystals) in the thin section containing plagioclase and pyroxenes (Figure 11).

The plagioclase depicted in figure 12 is a large anhedral phenocryst with mottled inclusions and zoning. Most of the plagioclase grains in this sample are anhedral to subhedral

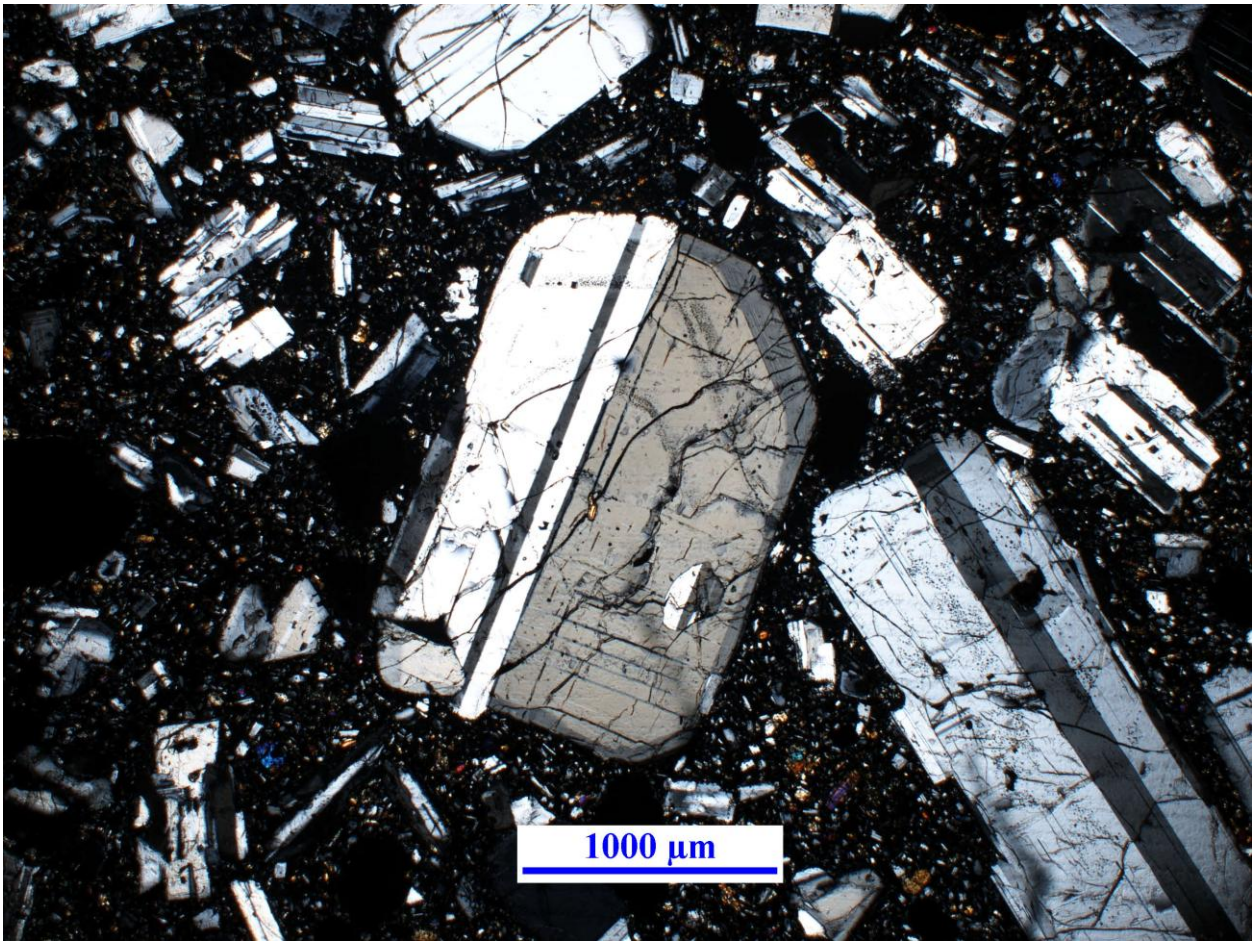

Figure 9: A euhedral plagioclase phenocryst with zoning and inclusions (CM-33).

with complex twinning patterns and zoning. Many of the inclusions are mottled, have non-spherical shapes, and do not exhibit obvious patterns.

Mutnovsky II

Sample CM-147 is a fine to medium-grained porphyritic andesite with hypocrystalline and flow-aligned texture. This thin section has only a few large phenocrysts (>1000 microns), unlike the other samples. The largest phenocryst in the sample is a plagioclase grain that is 2 millimeters in length. Most of this sample consists of tiny phenocrysts (nearly microphenocrystic

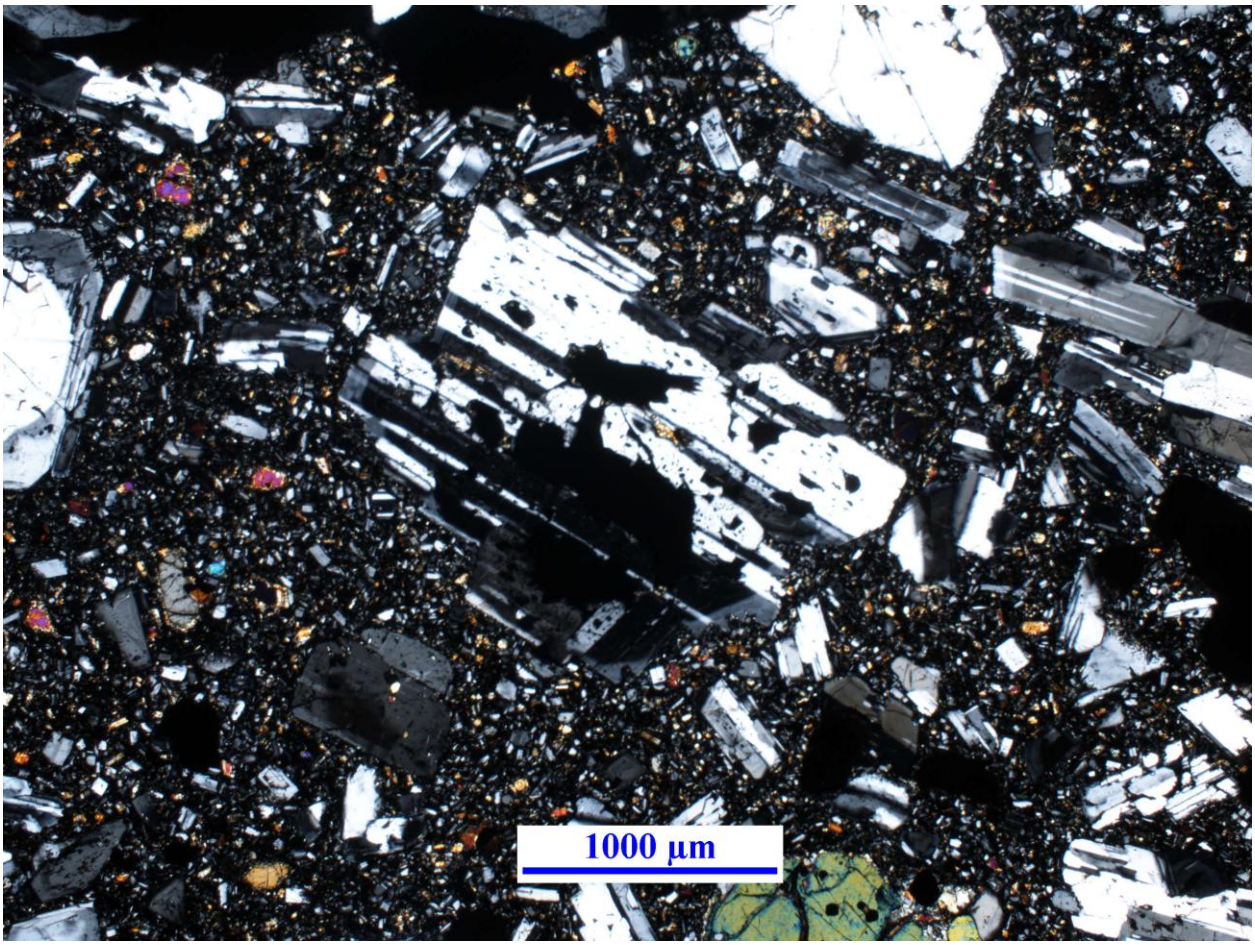

Figure 10: An anhedral plagioclase phenocryst with zoning and mottled inclusions (CM-33).

in size) of plagioclase and a glassy groundmass. The thin section consists of 87.2% groundmass and 12% plagioclase. The rest of the thin section is less than 1% pyroxenes and groundmass.

Many of the tiny phenocrysts of plagioclase, which make up the vast majority of the plagioclase in this sample, are elongate grains with swallowtail texture or other jagged terminations (Figure 13). The few larger phenocrysts of plagioclase have mottled inclusions and complex twinning patterns.

Sample CM-113 is a medium-grained porphyritic rhyodacite with hypocrystalline texture. The sample contains glomerocrysts and phenocrysts of plagioclase (13.7 %) and pyroxenes

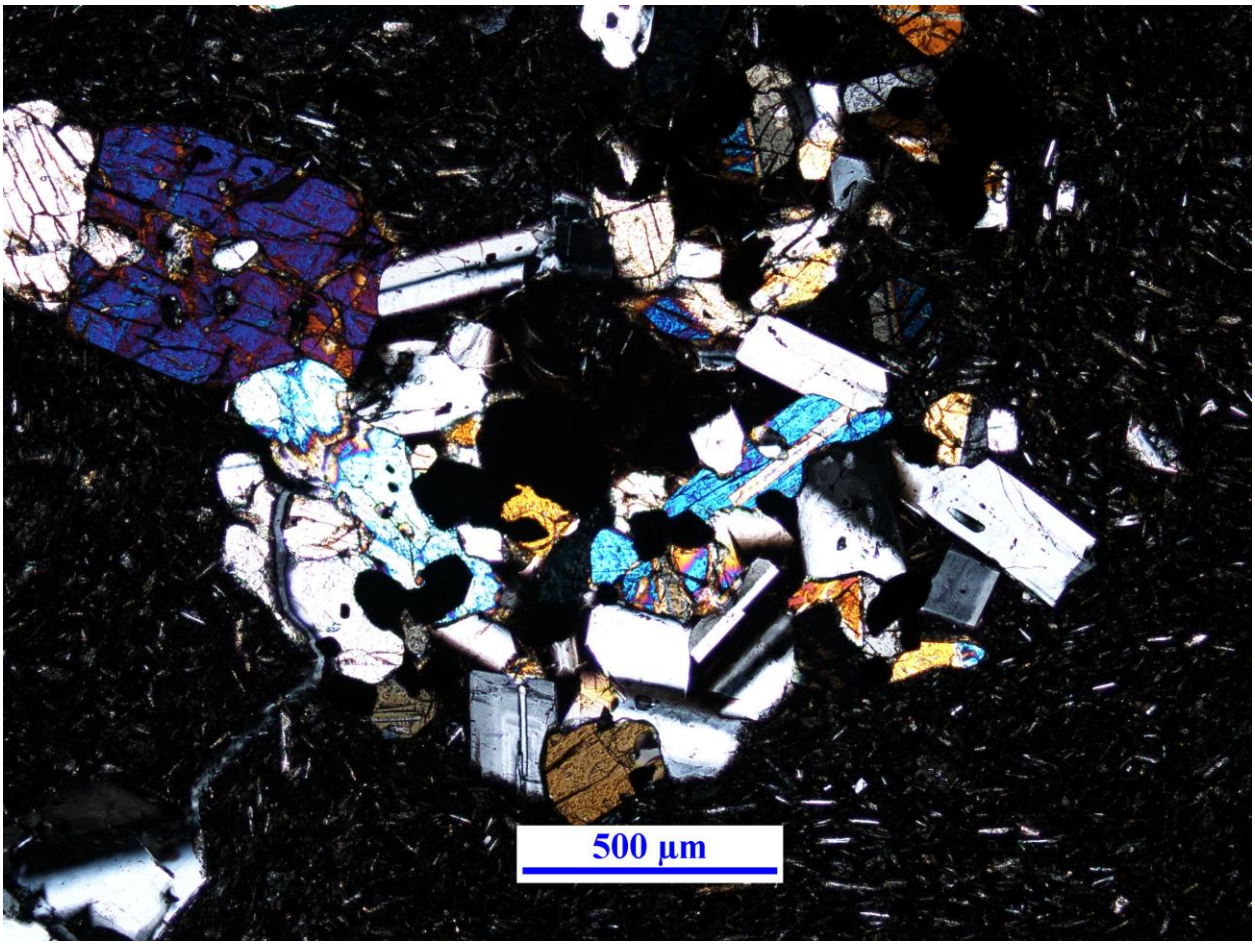

Figure 11: A glomerocryst containing plagioclase and clinopyroxene (CM-47).

(1.7%) suspended in a glassy, microlite-rich groundmass (80.7%). The SEM confirmed that there is trace quartz in the sample (less than 2%). The plagioclase phenocrysts in the sample can be approximately divided into two populations. Many of the largest phenocrysts are anhedral with complex twinning patterns and a mottled network of inclusions (Figure 14). In contrast, many of the smaller phenocrysts are euhedral and demonstrate simple twinning. Most of the plagioclase analyzed is oscillatory-zoned. One of the grains is reversely-zoned.

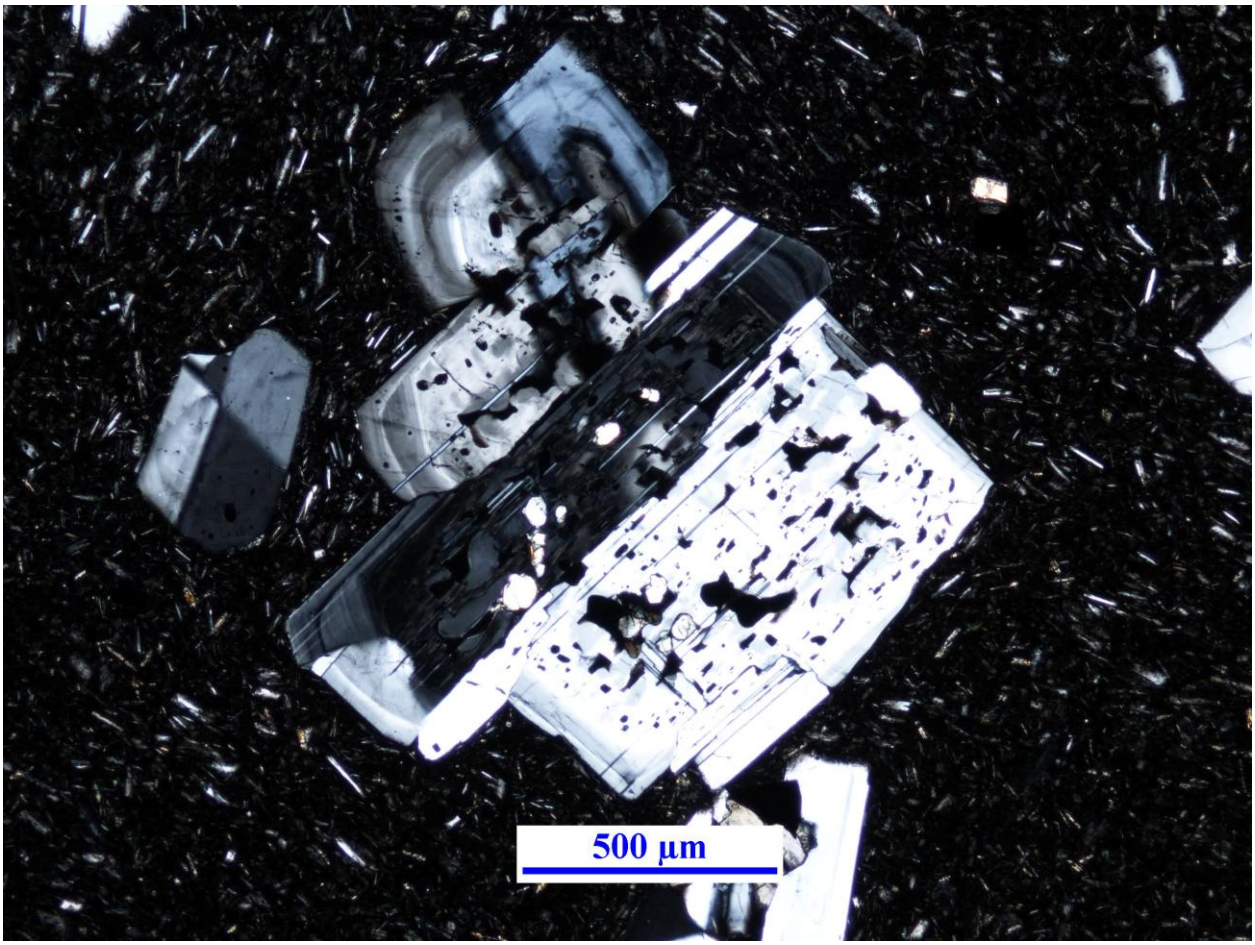

Figure 12: An anhedral plagioclase with mottled inclusions and zoning (CM-47).

Mutnovsky III

Sample M3-08-08 is a hypocrystalline and coarse-grained basalt. It is 65.4% groundmass and has phenocrysts of mostly plagioclase (30.8%) and olivine (3.4%) with some phenocrystic pryoxene (<1%). Most of the plagioclase exists as both large and small anhedral phenocrysts with mottled inclusions. There are also a few large euhedral phenocrysts of plagioclase with non-mottled tiny to medium-sized inclusions (Figure 15). These inclusions, in contrast to the CM-33 basalt, do not demonstrate clustering patterns that reflect the growth zones of the phenocryst; however, these inclusions seem confined to the core of the crystal.

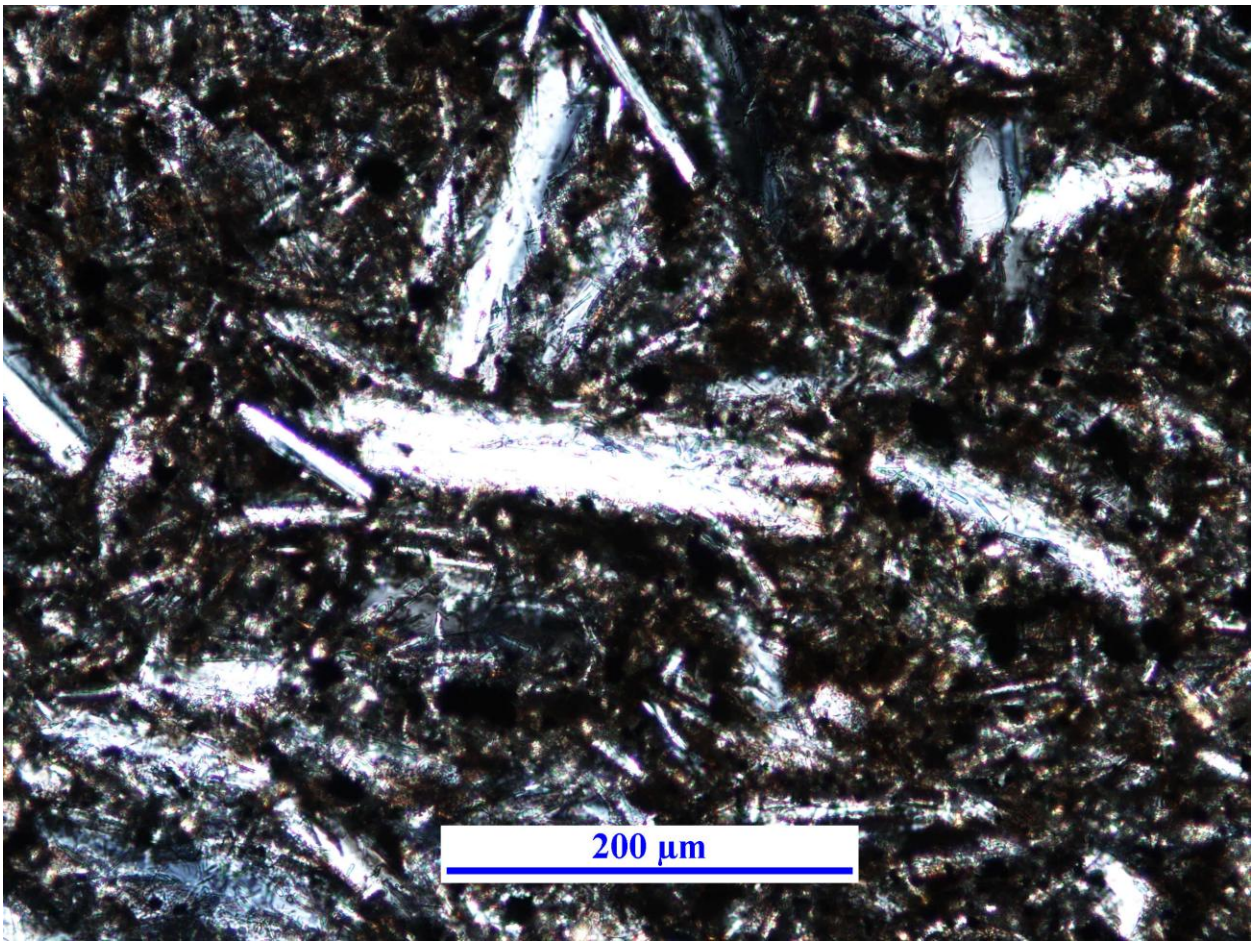

Figure 13: Swallowtail texture in a plagioclase microphenocryst(CM-147).

Sample CM-8a is a dacite that has similar texture to the dacite CM-47. It is hypocrystalline, porphyritic, and medium-grained, and it contains a glomerocryst. The groundmass is glassy with microlites, and it makes up 85.4% of the sample. There are phenocrysts of plagioclase (11.7%) and pyroxenes (1.1%). Most of the plagioclase phenocrysts. in this sample are euhedral and have simple twinning patterns and optical zoning. A significant portion of the plagioclase grains lack visually recognizable inclusions. There are two plagioclase grains that have a different texture from the majority of the plagioclase. These grains are anhedral, and they have complex twinning patterns and mottled inclusions (Figure 16). Most of the plagioclase in this sample is normally and oscillatory-zoned (Figure 17).

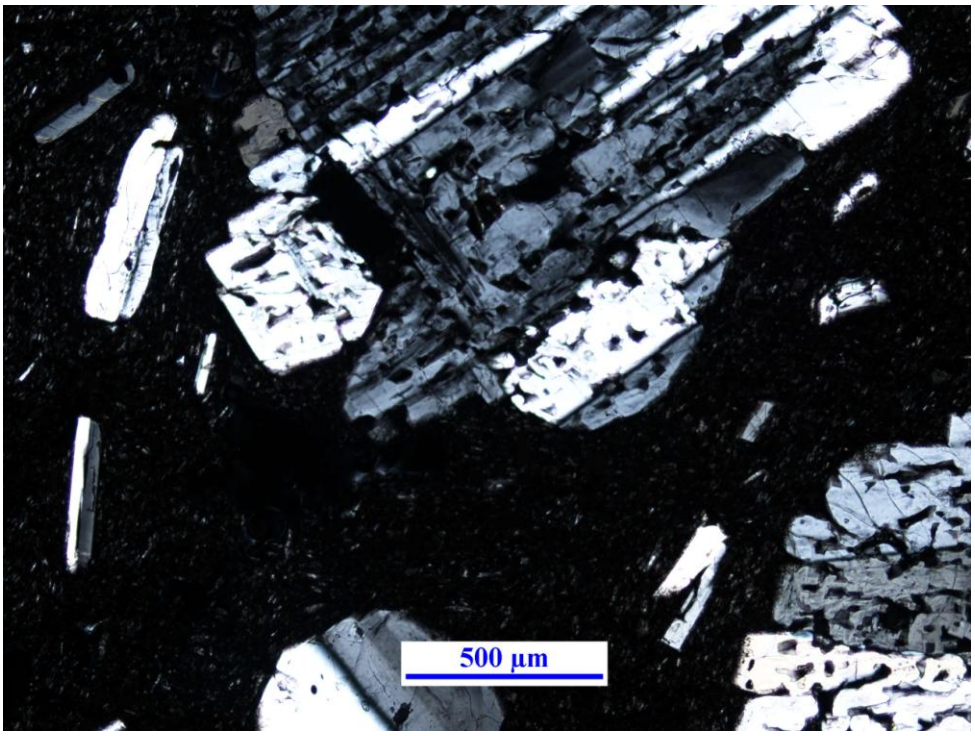

Figure 14: A large, anhedral plagioclase phenocryst with mottled texture and a small, euhedral plagioclase phenocrysts with simple twinning (CM-113).

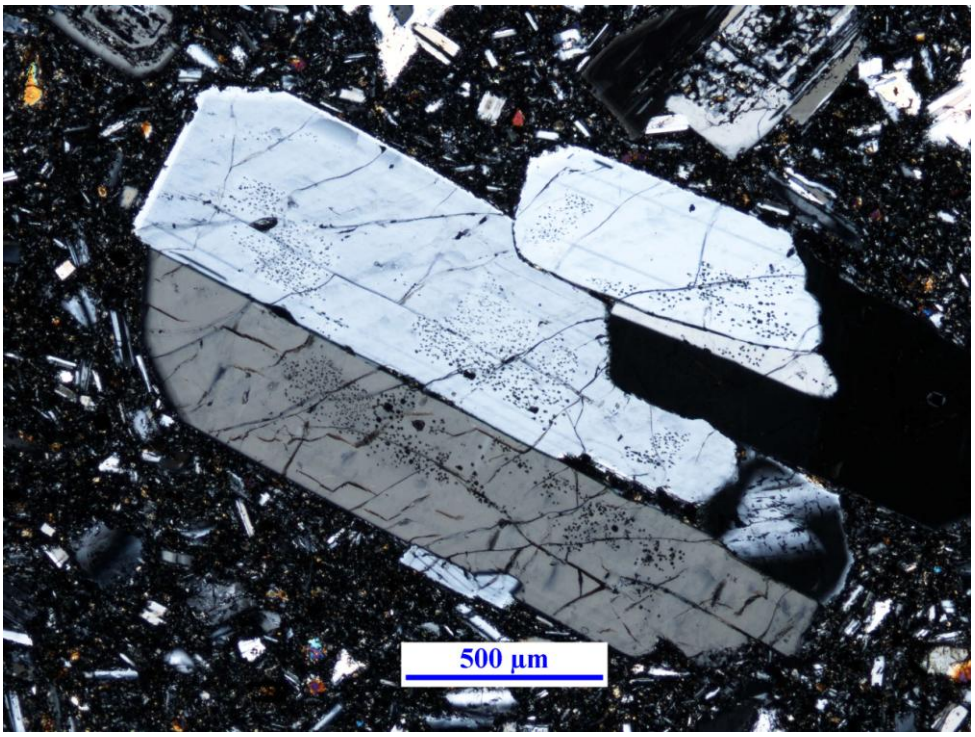

Figure 15: Plagioclase grains in M3-08-08 with tiny, non-mottled inclusions.

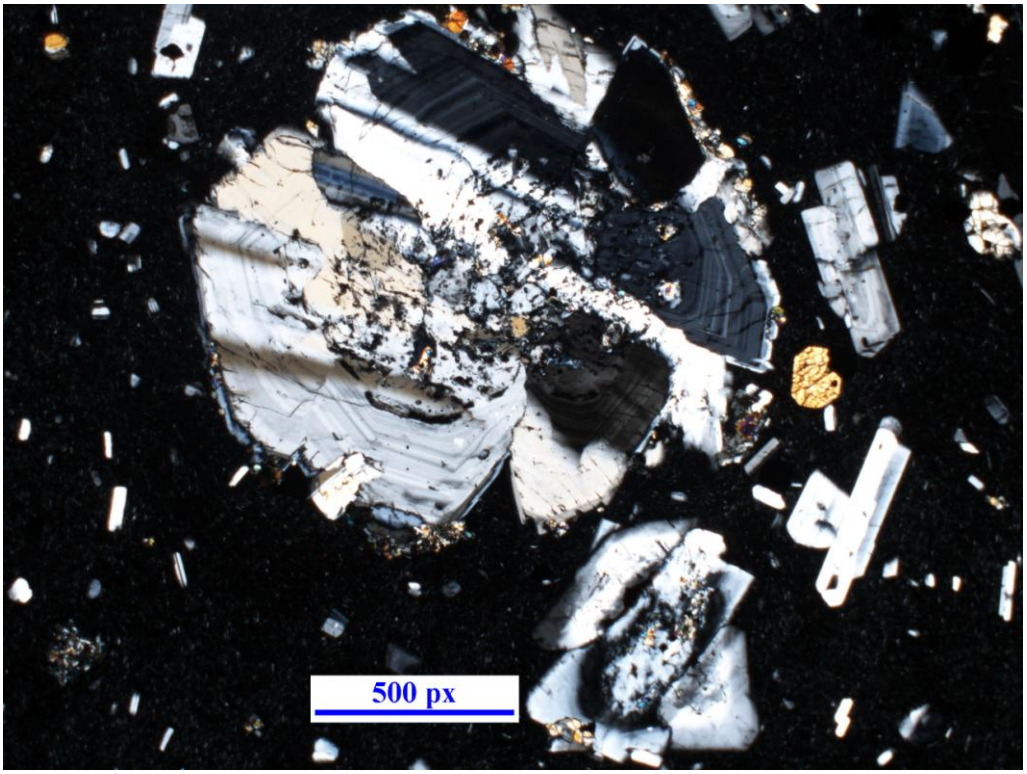

Figure 16: Two anhedral plagioclase grains in CM-8a with complex twinning patterns and mottled inclusions.

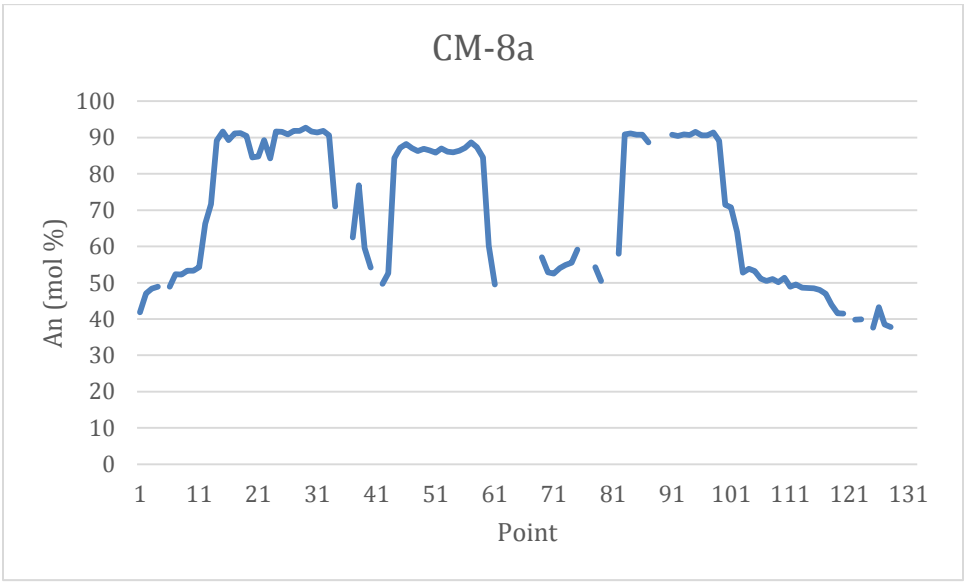

Figure 17: In CM-8a, an EPMA traverse of an oscillatory-zoned plagioclase grain.

Discussion

A plethora of published studies used plagioclase textures and compositions, modal mineralogy, and phenocryst and microphenocryst crystallinity to investigate magmatic processes (e.g., Churikova et al., 2007, Kent et al., 2010, Crabtree & Lange, 2010, Frey & Lange, 2011, and Innocent et al., 2013). This discussion consolidates the information from the literature and compares and contrasts the findings of numerous research groups with the data and observations from this study.

One hypothesis commonly discussed in the literature is that plagioclase textures and compositions are consistent with magma mixing, especially for the production of intermediate melt compositions such as andesite (e.g., Kent et al., 2010). Several papers described plagioclase textures that are characteristic of a magma mixing event. Churikova et al. (2007) studied plagioclase phenocrysts in a mafic enclave hosted in dacitic lava, and reported that the cores of these phenocrysts exhibit a sieve texture (Figure 3), which could be produced by magma mixing during the early growth stages of plagioclase. Their observation is consistent with plagioclase textures observed during the current study. For example, in CM-8a, the plagioclase grains in a dacite exhibit sieved cores (Figure 18). In addition, many of the Mutnovsky samples with andesitic or dacitic bulk composition exhibit a variety of disequilibrium textures, including sieve texture, skeletal texture, and ratty crystal boundaries. In the literature, disequilibrium textures are commonly invoked as evidence for magma mixing. Although many of our observations are consistent with the literature, there are differences.

One conflict that arises is that the observed modal mineralogy may be different from what would be expected if magma mixing were an important mechanism at Mutnovsky Volcano.

If these lavas were primary melts, the modal mineralogy would be expected to reflect the normative

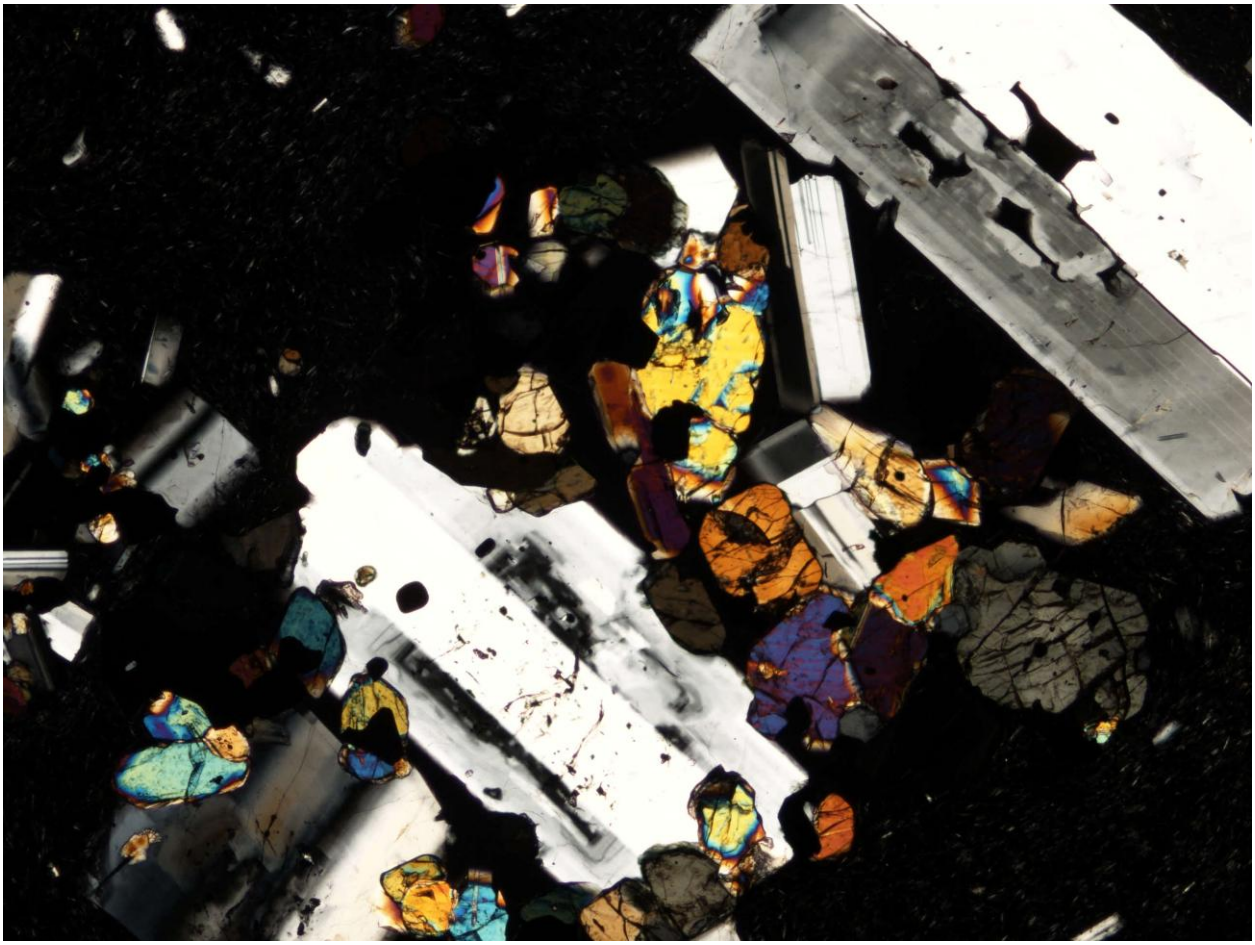

Figure 18: A sieved core in a plagioclase phenocryst, upper-right.

mineralogy. As such, we would expect some quartz but no olivine if these rocks crystallized fully. In contrast, if these lavas were produced by a mixing event, we would anticipate the quartz to coexist with some olivine. As previously mentioned, the SEM confirmed that quartz is present in the dacitic and rhyodacitic samples; however, olivine is not present.

Although Reubi & Blundy (2009) focus on melt inclusion data, they mention an observation that conflicts with the observations from the current study. Like Churikova et al. (2007), Reubi & Blundy (2009) explain that crystals in andesites that form by mixing silicic and

mafic magmas are typically characterized by disequilibrium textures. While their observations are consistent with ours, it is also true that we observed disequilibrium texture across the compositional range of the samples from Mutnovsky. We found sieve-textured plagioclase in samples with bulk compositions including basalt, andesite, and dacite. Robertson et al. (2013) reported that sieve texture can result from rapid decompression, highlighting that a number of factors in addition to magma mixing can explain the textures found in these samples.

In their study of phenocryst-poor andesites and dacites from a monogenetic peripheral vent, Crabtree and Lange (2010) also described plagioclase textures and compositions. These authors, in contrast to that of Churikova et al. (2007) and others, focused on the role that degassing-induced crystallization plays in producing complex plagioclase textures. They observed swallowtail, skeletal, and hopper textures in plagioclase phenocrysts as well as large interior melt hollows in some grains. They explained that these textures are characteristic of diffusion-limited growth caused by large undercoolings that occur when magmas degas. We found the textures described in both of these studies in volcanic rocks from Mutnovsky. For example, the rhyodacite sample contains many small grains (microphenocrysts) with large interior melt follows (Figure 19). As described in the results section, we also observed swallowtail texture in small phenocrysts (about 200 microns each in size) in the andesite sample (Figure 13). Finally, there is a notable absence of hydrous phases such as amphibole across all of the samples, which suggests that degassing may have produced the observed textures. Nevertheless, we still discovered several inconsistencies when we continued to compare the results of this study with those of Crabtree & Lange (2010) and Frey & Lange (2011). For example, Frey & Lange (2011) discuss patterns in plagioclase compositions to support the model of degassing-induced crystallization over magma mixing. In their study, they found that the

plagioclase in andesites and dacites display a wide, continuous range in anorthite content. They invoke this compositional variation of plagioclase as evidence for a loss of dissolved water

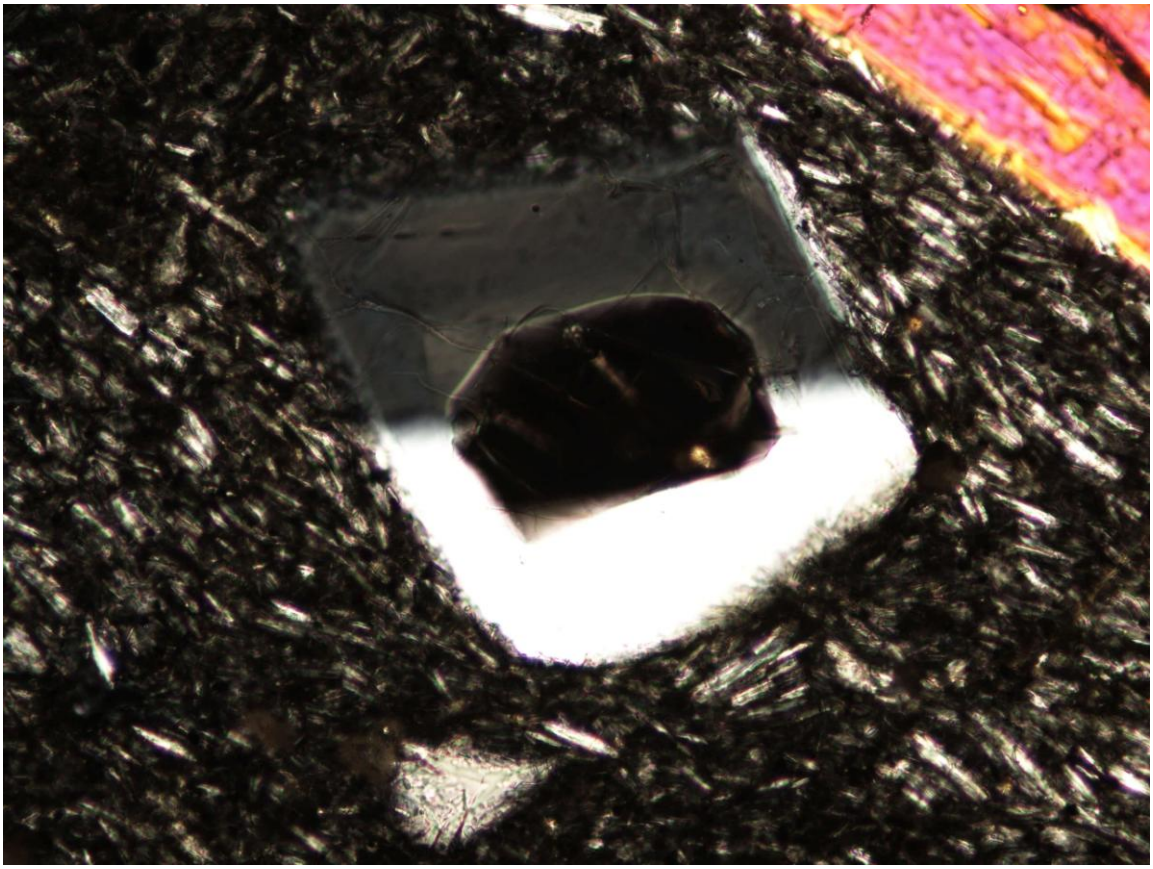

Figure 19: A large interior melt hollow in a plagioclase microphenocryst (20X, XPL).

from the melt during degassing. In contrast to the results of Frey & Lange (2011) in this study many of the plagioclase grains in the dacites and in other samples have bimodally distributed anorthite contents (Figure 20). A degassing-induced crystallization model does not explain the observed bimodal distribution, and it is traditionally cited as evidence for magma mixing.

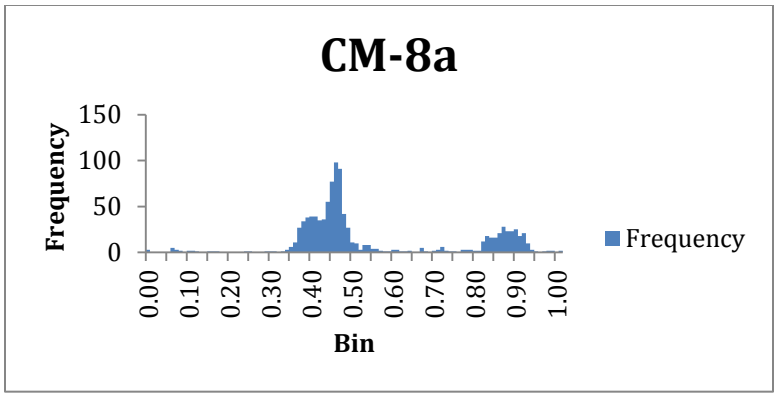

Figure 20: Variation of anorthite content in plagioclase from a dacite.

Another observation that is seemingly inconsistent with the degassing-induced crystallization model is the variety of plagioclase textures and compositions we observed within one sample. Recall that in CM-33, we observed both euhedral plagioclase and sieve-textured anhedral plagioclase within one thin section. This observation was common across all Mutnovsky samples. In addition, the plagioclase traverses revealed the coexistence of normally-zoned plagioclase, reversely-zoned plagioclase, and sometimes even oscillatory-zoned plagioclase, as in the dacite sample CM-8a. If degassing were the primary mechanism producing the zoning disequilibrium textures we observed, we would expect more textural and compositional uniformity within the samples. Therefore, it is necessary to understand if and how degassing can produce such textural and chemical diversity in one sample.

Conclusions

1. The types of textures observed in the Mutnovsky samples are consistent with observations in the literature, and they suggest that the crystals experienced disequilibrium and/or diffusion-limited growth prior to eruption. The lack of amphibole across the samples is potential evidence for a degassing-induced crystallization model.

2. One problem with the degassing-induced crystallization model is that it cannot explain the diversity of textures and compositions observed within individual samples, which are consistent with the magma mixing model.
3. Nevertheless, magma mixing is not a perfect solution at Mutnovsky Volcano for two main reasons. First, we were unable to confirm the coexistence of quartz and olivine in any of the Mutnovsky samples, which is important evidence for magma mixing. Second, the expectation is that magma mixing to produces disequilibrium textures primarily in intermediate magmas; however, there was no evidence in the Mutnovsky samples that suggested the crystals in the intermediate magmas had significantly more disequilibrium texture compared to the crystals in the end-member magmas.
4. There is no unequivocal evidence that allows us to eliminate either magma mixing or degassing-induced crystallization as a model for Mutnovsky Volcano. Instead the results from this study force us to conclude that the most likely scenario for Mutnovsky Volcano includes a combination of processes, including magma mixing, degassing-induced crystallization, and potentially others not discussed in this study, which collectively produce the textural and chemical diversity observed in the samples.

Acknowledgments

I would like to thank Dr. Adam Simon for allowing me to work in his lab and for his guidance throughout the project. Tom Hudgins provided the EPMA data and training for the petrographic microscope and SEM. Finally, I thank Dr. Gordon Moore and the Electron Microprobe Analysis Laboratory (EMAL) for providing access to their equipment.

References

Churikova, T., Worner, G., Eichelberger, J., & Ivanov, B. (2007). Minor and trace element zoning in plagioclase from kizimen volcano, kamchatka: Insights on the magma chamber

processes .*Volcanism and Subduction: The Kamchatka Region* , 303-323. doi: 10.1029/172GM22

Couch, S., Sparks, R. S. J. & Carroll, M. R. (2003). The kinetics of degassing-induced crystallization at Soufrie' re Hills Volcano, Montserrat. Journal of Petrology 44, 1477^1502.

Crabtree, S. M., & Lange, R. A. (2010). Complex phenocryst textures and zoning patterns in andesites and dacites: evidence of degassing-induced rapid crystallization?. *Journal of Petrology, 52*(1), 3-38. doi: doi:10.1093/petrology/egq067

Frey, H. M., & Lange, R. A. (2011). Phenocryst complexity in andesites and dacites from the tequila volcanic field, mexico: resolving the effects of degassing vs. magma mixing.*Contributions to Mineralogy and Petrology* , 415-445. doi: 10.1007/s00410-010-0604-1

Hammer, J. E. & Rutherford, M. J. (2002). An experimental study of the kinetics of decompression-induced crystallization in silicic melt. Journal of Geophysical Research 107(BI), 2021.

Innocenti, S., del Marmol, M., Voight, B., Andreastuti, S., & Furman, T. (2013). Textural and mineral chemistry constraints on evolution of merapi volcano, indonesia. *Journal of Volcanology and Geothermal Research, 261*, 20-37.

Johannes W, Koepke J, Behrens H (1994) Partial melting reactions of plagioclase and plagioclase-bearing assemblages. In: Parson I (ed) Feldspars and their reactions. Kluwer, Dordrecht, pp 161–194

Kent, A. J., Darr, C., Koleszar, A. M., Salisbury, M. J., & Cooper, K. M. (2010). Preferential eruption of andesitic magmas through recharge filtering.*Nature Geoscience, 3*, 631-636.

Lofgren, G. (1974). An experimental study of plagioclase crystal morphology: isothermal crystallization. American Journal of Science 274, 243^273.

Martel, C. & Schmidt, B. C. (2003). Decompression experiments as an insight into ascent rates of silicic magmas. Contributions to Mineralogy and Petrology 144, 397^415.

Moore GW, Bogdanov NA, Drummond KJ, Golovchenko X, Larson RL, Pitman WC III, Rinehart WA, Siebert L, Simkin T, Tilman SM, Uyeda S (1992) Plate-tectonic map of the Circum- Pacific Region, Arctic Sheet, in Circum-Pacific Map Series, pp. 20, United States Geological Survey.

Reubi, O., & Blundy, J. (2009). A dearth of intermediate melts at subduction zone volcanoes and the petrogenesis of arc andesites. *Nature, 461*, 1269-1274. doi: 10.1038/nature08510

Robertson, K., Simon, A., Pettke, T., Smith, E., Selyangin, O., Kiryukhin, A., Mulcahy, S. R., & Walker, J. D. (2013). Melt inclusion evidence for magma evolution at mutnovsky volcano, kamchatka. *Geofluids*, *13*(4), 421-439. doi: 10.1111/gfl.12060

Selyangin, O. B. (1993). Mutnovskiy volcano, kamchatka: New evidence on structure, evolution, and future activity . *Volcanology and Seismology*, *15*(1), 17-38.

Suzuki, Y., Gardner, J. E. & Larsen, J. F. (2007). Degassing and micro- lite crystallization of basaltic andesite magma erupting at Arenal volcano, Costa Rica. Journal of Volcanology and Geothermal Research 157, 182^201.

Szramek, L., Gardner, J. E. & Larsen, J. F. (2007). Experimental constraints on syn-eruptive magma ascent related to the phreato- magmatic phase of the 2000 AD eruption of Usu Volcano, Japan. Bulletin of Volcanology 69, 423^444.